

Accepted Manuscript

Design, synthesis, molecular docking and biological evaluation of thiophen-2-iminothiazolidine derivatives for use against *Trypanosoma cruzi*

E.F. Silva-Júnior, E.P.S. Silva, P.H.B. França, J.P.N. Silva, E.O. Barreto, E.B. Silva, R.S. Ferreira, C.C. Gatto, D.R.M. Moreira, J.L. Siqueira-Neto, F.J.B. Mendonça-Júnior, M.C.A. Lima, J.H. Bortoluzzi, M.T. Scotti, L. Scotti, M.R. Meneghetti, T.M. Aquino, J.X. Araújo-Júnior

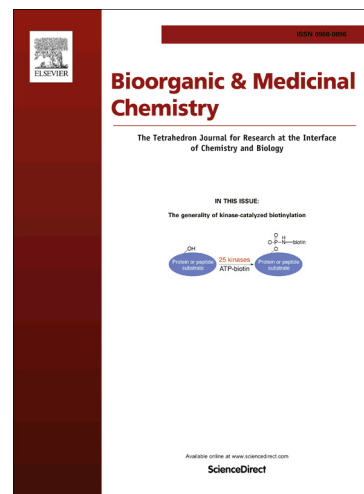
PII: S0968-0896(16)30505-3
DOI: <http://dx.doi.org/10.1016/j.bmc.2016.07.013>
Reference: BMC 13126

To appear in: *Bioorganic & Medicinal Chemistry*

Received Date: 14 June 2016
Revised Date: 6 July 2016
Accepted Date: 8 July 2016

Please cite this article as: Silva-Júnior, E.F., Silva, E.P.S., França, P.H.B., Silva, J.P.N., Barreto, E.O., Silva, E.B., Ferreira, R.S., Gatto, C.C., Moreira, D.R.M., Siqueira-Neto, J.L., Mendonça-Júnior, F.J.B., Lima, M.C.A., Bortoluzzi, J.H., Scotti, M.T., Scotti, L., Meneghetti, M.R., Aquino, T.M., Araújo-Júnior, J.X., Design, synthesis, molecular docking and biological evaluation of thiophen-2-iminothiazolidine derivatives for use against *Trypanosoma cruzi*, *Bioorganic & Medicinal Chemistry* (2016), doi: <http://dx.doi.org/10.1016/j.bmc.2016.07.013>

This is a PDF file of an unedited manuscript that has been accepted for publication. As a service to our customers we are providing this early version of the manuscript. The manuscript will undergo copyediting, typesetting, and review of the resulting proof before it is published in its final form. Please note that during the production process errors may be discovered which could affect the content, and all legal disclaimers that apply to the journal pertain.





Design, synthesis, molecular docking and biological evaluation of thiophen-2-iminothiazolidine derivatives for use against *Trypanosoma cruzi*

Silva-Júnior, E.F.^a, Silva, E.P.S.^a, França, P.H.B.^a, Silva, J.P.N.^b, Barreto, E.O.^b, Silva, E.B.^c, Ferreira, R.S.^c, Gatto, C.C.^d, Moreira, D.R.M.^e, Siqueira-Neto, J.L.^f, Mendonça-Júnior, F.J.B.^g, Lima, M.C.A.^h, Bortoluzzi, J.H.ⁱ, Scotti, M.T.^g, Scotti, L.^g, Meneghetti, M.R.ⁱ, Aquino, T.M.^{*a}, Araújo-Júnior, J.X.^a

^aMedicinal Chemistry Laboratory, Pharmacy and Nursing School, Federal University of Alagoas, Maceio, Brazil

^bCell Biology Laboratory, Federal University of Alagoas, Maceio, Brazil

^cBiochemistry and Immunology Department, Biological Sciences Institute, Federal University of Minas Gerais, Belo Horizonte, Brazil

^dInorganic Synthesis and Crystallography Laboratory, Institute of Chemistry, University of Brasília, Federal District, Brazil

^eTissue Engineering and Immunopharmacology Laboratory, Oswaldo Cruz Foundation, Salvador, Bahia, Brazil

^fSkaggs School of Pharmacy and Pharmaceutical Sciences, California, San Diego La Jolla, United States of America

^gLaboratory of Drug Synthesis and Delivery, Biological Sciences Department, State University of Paraíba, Campus V, João Pessoa, Brazil

^hDrug Design and Synthesis Laboratory, National Science and Technology Institute for Pharmaceutical Innovation, Federal University of Pernambuco, Recife, Brazil

ⁱCatalysis and Chemical Reactivity Group (GCaR), Institute of Chemistry and Biotechnology, Federal University of Alagoas, Maceio, Brazil

ARTICLE INFO

Article history:

Received

Received in revised form

Accepted

Available online

Keywords:

Thiophene

Thiazolidine

Docking

T. cruzi

Chagas disease

ABSTRACT

In this study, we designed and synthesized a series of thiophen-2-iminothiazolidine derivatives from thiophen-2-thioureic with good anti-*Trypanosoma cruzi* activity. Several of the final compounds displayed remarkable trypanocidal activity. The ability of the new compounds to inhibit the activity of the enzyme cruzain, the major cysteine protease of *T. cruzi*, was also explored. The compounds **3b**, **4b**, **8b** and **8c** were the most active derivatives against amastigote form, with significant IC₅₀ values between 9.7 and 6.03 μM. The **8c** derivative showed the highest potency against cruzain (IC₅₀ = 2.4 μM). Molecular docking study showed that this compound can interact with subsites S1 and S2 simultaneously, and the negative values for the theoretical energy binding (Eb= -7.39 kcal·mol⁻¹) indicates interaction (via dipole-dipole) between the hybridized sulfur sp³ atom at the thiazolidine ring and Gly66. Finally, the results suggest that the thiophen-2-iminothiazolidines synthesized are important lead compounds for the continuing battle against Chagas disease.

2016 Elsevier Ltd. All rights reserved.

1. Introduction

Neglected tropical diseases (NTDs) are a diverse group of diseases that prevail in tropical and subtropical countries and are responsible for causing illness in more than 1 billion people around the world. It has been estimated that around 8 million of these cases are associated with the parasite *Trypanosoma cruzi*, which causes Chagas disease [1–3]. This disease is controlled at present through the elimination of the vectors with the use of insecticides and the serological screening of blood. Better housing and educational campaigns are also fruitful approaches. As with other parasitic diseases, this pathology is associated with poverty and low educational levels [4]. Current chemotherapy for Chagas disease is unsatisfactory due to its limited efficacy, particularly in the chronic phase, with frequent side effects that can lead to the discontinuation of treatment [5]. The development of resistance by some strains of *T. cruzi* toward gold-standard

drugs, such as nifurtimox and benznidazole (Fig. 1), represents a serious public health problem [2]. Also, these drugs present disadvantages that limit their use: they produce active metabolites which to interact with the DNA of the host leading to deleterious effects, such as cancer [6,7], resistance, lack of efficacy in the late-stage of the disease and a lack of pediatric formulations [8]. The survival of *T. cruzi* in the cells of the host is guaranteed by important enzymes (e.g. cruzain) which play a role in different processes including absorption, penetration, survival, infectivity, immune evasion, nutrition and growth [6].

Cruzain is a cathepsin-L-like protease (also known as cysteine protease) of the papain family. It is thought to be essential for the infection of host cells and the replication and metabolism of the parasite and it plays multiple roles in the disease pathogenesis [4,5]. Furthermore, the selective inhibition of cysteine proteases as a therapeutic target has transcended the laboratory to the clinic. Recently, odanacatib (Fig. 1), a drug based on cysteine protease inhibition, has shown high efficacy and a good safety

profile in Phase III clinical trials. Also, many studies in animal models have validated the use of this enzyme for the control and elimination of *T. cruzi* [8].

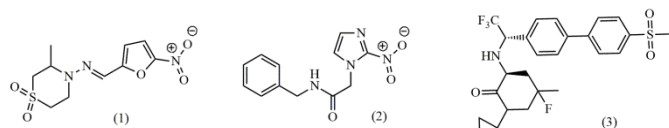


Figure 1. Structures of nifurtimox (1), benznidazole (2) and odanacatib (3).

Many thiophene compounds have been described as very active derivatives against *T. cruzi* (Fig. 2) and these are interesting starting materials for new therapeutic agents [9]. The thiophene aromatic ring is a hydrophobic site which binds to the hydrophobic-pockets in some enzymes [10].

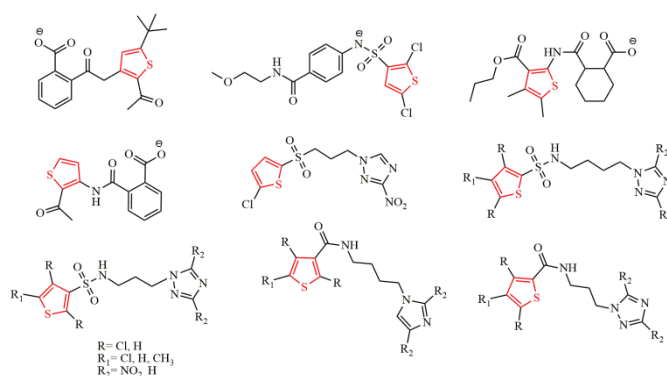


Figure 2. Some thiophene derivatives described in the literature which are active against *Trypanosoma cruzi*.

The pharmacological activity of thiazolidine compounds is of current interest. Thiazolidine and its hybrids have been reported to possess promising anticancer and antiviral properties. In addition, the thiazolidine scaffold is extremely important in the design and synthesis of novel biologically active agents with action against *Trypanosoma spp.* [11]. Many compounds with the thiazolidine ring in their structure (Fig. 3) have been described in the literature and they show promising anti-*T. cruzi* activity [1,5,6,11].

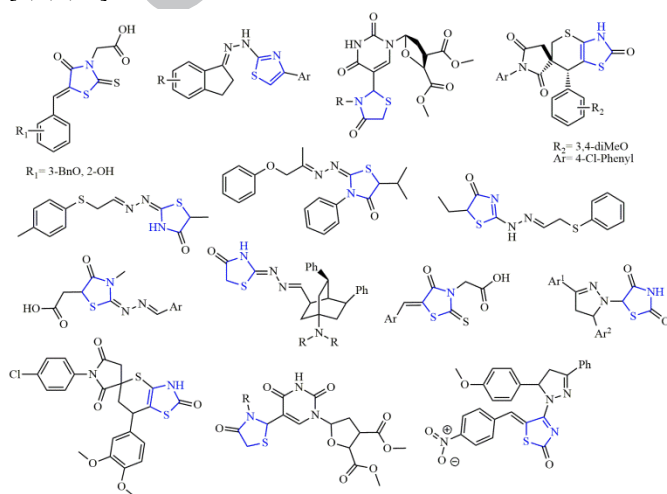


Figure 3. Some thiazolidine derivatives described in literature which are active against *Trypanosoma cruzi*.

In this study, we synthesized new thiophene-thiazolidine hybrid derivatives bearing various groups at the thiazolidine ring, with a linker (imine group) between the thiophene and thiazolidine rings (Fig. 4). All derivatives were tested for their ability to inhibit the in vitro growth of amastigote and trypomastigote forms of *Trypanosoma cruzi* and the activity of the enzyme cruzain. In addition, we carried out theoretical studies involving molecular docking simulations and pharmacophoric identification.

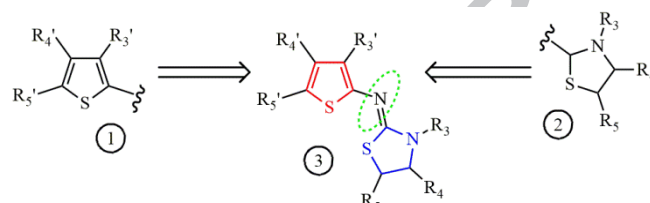
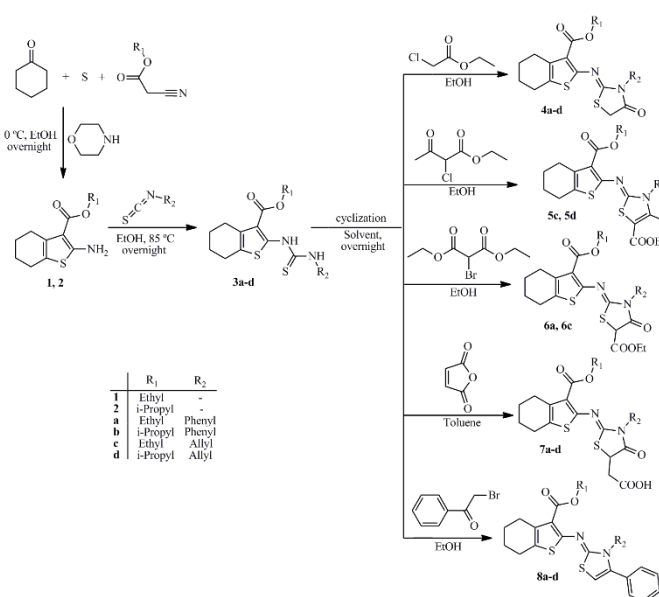


Figure 4. Molecular hybridization pathway for the synthesis of the compounds. 1: thiophene ring; 2: thiazolidine ring; 3: hybrid scaffold. Imine bond as linker shown in green.

2. Results and Discussion

2.1. Chemistry

The 2-aminothiophene analogues (**1**, **2**) were readily prepared via the Gewald reaction, a multicomponent synthesis involving an aldehyde or ketone, an activated nitrile and elemental sulfur [12–14]. The intermediates (**3a-d**) were then synthesized through the treatment of **1** or **2** with substituted isothiocyanates (phenyl and allyl). Spectral analysis for these compounds was carried out according to methods described in the literature [13,15]. Finally, thiophen-2-iminothiazolidines were prepared via thia-Michael cyclization (**7a-d**) or substitution followed by intramolecular cyclization (**4a-d**, **5c**, **d**, **6a**, **6c** and **8a-d**) between thiophen-2-thiourea and dielectrophiles [16,17]. All of these reactions proceeded well with refluxing overnight. The synthetic route is shown in Scheme 1. Four compounds previously designed were not included in this work (two cyclization using ethyl 2-chloroacetate and two using 2-bromomalonate) due the formation of many secondary products and impossibility of purification by



recrystallization or flash column chromatography.

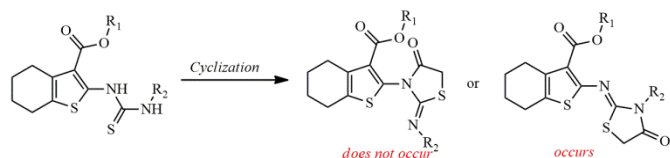
Scheme 1. Synthetic route for thiophen-2-thiourea and thiophen-2-iminothiazolidine derivatives.

The structures of the new compounds synthesized were established by ^1H and ^{13}C 1D and 2D NMR analysis. For the final compounds, in ^1H NMR spectra, signs of the protons from thiourea moiety of **3a-d** signs were not displayed, and peaks resonated at 154.48-158.49 and 158.32-163.94 ppm in the ^{13}C NMR spectra were respectively assigned to C-4 and C-2 of the thiazolidine ring. For compounds **4a-d** the ^1H NMR spectra revealed the presence of a singlet for thiomethylene protons at 3.66-3.90 ppm. In addition, ^{13}C NMR spectra exhibited resonated peaks for the same moiety at 33.39-34.97 ppm, as well as signals at 155.86-158.49 and 161.99-163.60 ppm assigned to C=N and C=O moieties, respectively. For compounds **5c** and **5d**, resonated peaks at 2.57-2.60 ppm in the ^1H NMR were attributed to substituent methyl groups at C-4 of thiazolidine ring and whose carbons appeared at 12.85-12.90 ppm in the ^{13}C NMR spectra. Compounds **6a**, **6c**, **7a-d** and **8a-d** may be distinguished by the resonated peaks of SCH moiety, which appears as a singlet at 5.28-6.08 ppm in ^1H NMR of derivatives **6a** and **6c**. On the other hand, for compounds **7a-d** the ^1H NMR spectra exhibited resonance assigned to the SCH group appearing as doublet at 4.39-4.53 ppm, due to the interaction with methylene protons of the acetyl group substituent at C-5 of the 4-thiazolidinone ring. For these compounds, the SCH moiety ranges from 43.81 to 59.94 ppm in the ^{13}C NMR. Lastly, compounds **8a-d** show resonated peaks for SCH further displaced downfield, with ^{13}C NMR signals being shown at 99.11-100.49 ppm.

The mechanism of thiazolidine ring formation is not well understood, which has led to erroneous proposal of structures obtained through the reaction of thiourea analogues with α -halo esters or acids in the presence of an inorganic base [18]. In the synthesis of **7a-d**, for example, it is accepted that this reaction begins with a nucleophilic attack by the sulfur atom of the thiourea on the C=C bond of maleic anhydride, followed by a proton transfer and a nucleophilic attack of a nitrogen atom on any of the two carbonyl groups, providing a five-membered 4-oxo-1,3-thiazolidine ring. Finally, aminolysis of this product occurs, giving the final compound with an acid function [19,20]. In ethanol reflux this reaction leads to many collateral products. Therefore, an aprotic solvent, such as toluene, was employed and satisfactory yields were obtained.

The general mechanism suggested is that the sulfur atom (soft nucleophile) of the thiourea will preferentially attack the α -halo esters (soft electrophile) and the NH (hard nucleophile) will attack the carbonyl center (hard electrophile) [18]. However, the regioselectivity of the nucleophilic attack from the non-equivalent nitrogen atoms of the thiourea still needs to be studied [20]. For unsymmetrical thioureas ($R_1 \neq R_2$), regiocontrol in the cyclization step is typically influenced by electronic factors that predispose electron-withdrawing substituents (i.e., aryl or heteroaryl groups) to maintain conjugative stabilization with the imine nitrogen [21].

In the case of the thiophen-2-iminothiazolidines described herein, the results of analysis using heteronuclear multiple bond correlation (HMBC) (see Fig. 5 for **4c** and supplementary data for the other compounds containing an allyl group) techniques support our conclusions regarding the position of the thiazolidine ring and the possibility of the existence of an ambiguous synthetic route is discarded (Scheme 2).



Scheme 2. Example of possible ambiguous synthetic route for thiophen-2-iminothiazolidines **4a-d**.

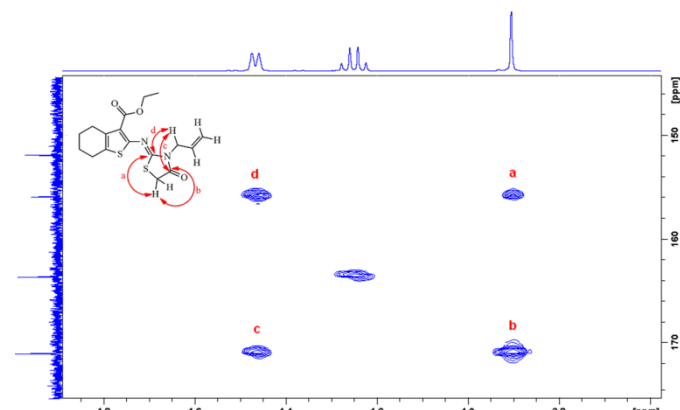
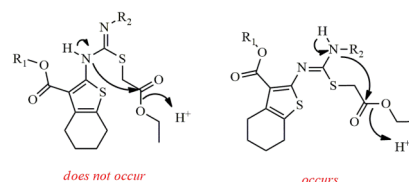


Figure 5. Thiazolidine ring conformation in 2D HMBC spectrum for **4c**.

Additionally, we performed a molecular modeling study using the structures of the intermediary and transition state of the synthetic route for compounds **3a** to **4a** (Scheme 3). A lower transition state energy value and, consequently, a smaller energy difference value for the intermediary of this route, verify that this is a favorable synthetic route for obtaining the product formed (Table 1). Also, the HOMO and LUMO energy gaps of both intermediaries were calculated and the energy gap value for ethyl 2-[[N-[3-(1-ethoxyethenyl)-4,5,6,7-tetrahydro-1H-inden-2-yl]-N'-phenylcarbamimidoyl]sulfanyl]acetate ($385.52 \text{ kJ}\cdot\text{mol}^{-1}$) is higher than that for ethyl 2-[[N-[3-(1-ethoxyethenyl)-4,5,6,7-tetrahydro-1H-inden-2-yl]-N-phenylcarbamimidoyl]sulfanyl]acetate ($370.46 \text{ kJ}\cdot\text{mol}^{-1}$). Therefore, the HOMO-LUMO interactions of the latter are stronger than those of the former, corroborating with the results obtained for the transition state energies and from the spectral data.



Scheme 3. Transition states of synthetic route for thiophen-2-iminothiazolidines (**4a-d**).

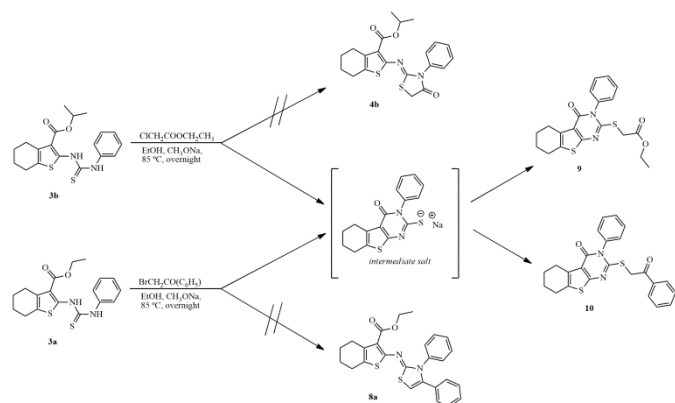
Table 1. Energies of intermediaries and respective transition states of possible ambiguous synthetic route for thiophen-2-iminothiazolidines (**4a-d**).

Intermediary	I^a	TS^b	$\Delta = TS - I^c$
	-5,410,603.0	-5,386,356.8	24,246.2
	-5,410,565.8	-5,386,457.6	24,108.3

^a: Intermediary energy; ^b: Transition state energy; ^c: Energy difference.

In an attempt to improve the yield for the cyclization, the synthesis of **4b** and **8a** were chosen, and sodium acetate was used as a catalyst. However, it was observed that this did not lead to the formation of the desired compound (Scheme 4), since the base deprotonates the nitrogen neighboring to the phenyl group

which, in turn, attacks the carbonyl of the ester group, closing the ring and providing the monosodium salt of the corresponding thienopyrimidine. Finally, thienopyrimidine salt reacts with the electrophile, leading to **9** and **10** as final products. The reason for this is that thienopyrimidines can be obtained from thiourea derivatives using a base salt [22–24]. Compound **9** was obtained as colorless crystals and its structure was confirmed by X-ray crystallography (Fig. 6A; Table 2). Yellow crystal of the compound **8b**, obtained from cyclization without sodium acetate, is shown in figure 6B, as well crystal data and structure refinement are described in table 2.



Scheme 4. Synthetic routes for the compounds **9** and **10**.

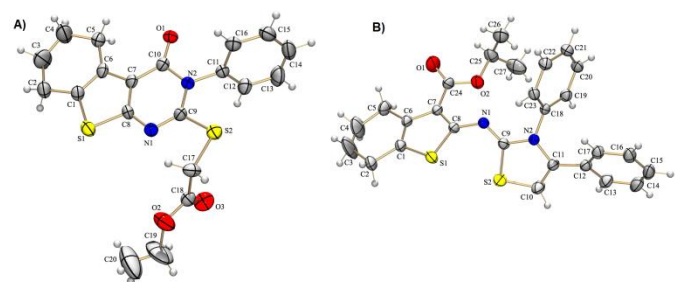


Figure 6. ORTEP view of compounds **9** (A) and **8b** (B).

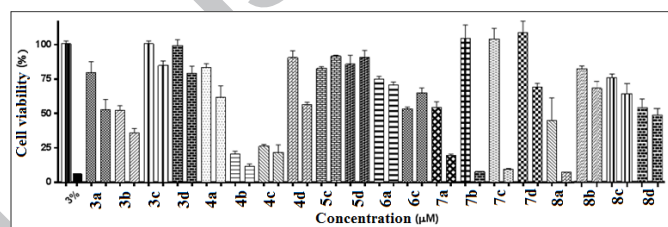
Table 2. Crystal data and structure refinement for **9** and **8b**.

Empirical formula	C ₂₀ H ₂₀ N ₂ O ₃ S ₂	C ₂₇ H ₂₆ N ₂ O ₂ S ₂
Formula weight	400.5	474.62
Temperature (K)	296(2)	296(2)
Wavelength (Å)	0.71073	0.71073
Crystal system	Orthorhombic	Monoclinic
Space group	P 21 21 21	P 1 21/n 1
<i>Unit cell dimensions</i>		
<i>a</i> (Å)	4.9546(6)	10.3078(2)
<i>b</i> (Å)	13.3793(18)	15.8286(4)
<i>c</i> (Å)	29.523(5)	14.9372(4)
Volume (Å ³)	1957.1(5)	2437.02(10)
<i>Z</i>	4	4
ρ_{calc} (g·cm ⁻³)	1.359	1.294
μ (mm ⁻¹)	0.295	0.245
<i>F</i> (000)	840	1000
Crystal size (mm)	0.060 x 0.130 x 0.590	0.420 x 0.600 x 0.630
θ range (°)	1.38 to 26.39	1.87 to 27.37
Reflections collected	10738	24135
Independent reflections	3993	5508
Observed reflections [<i>I</i> > 2 σ (<i>I</i>)]	1568	3525
<i>R</i> _{int}	0.1086	0.0531
Refinement method	Full-matrix least-squares on	Full-matrix least-squares on

	<i>F</i> ²	<i>F</i> ²
Data/restraints/parameters	3993 / 0 / 246	5508 / 0 / 300
Goodness-of-fit on <i>F</i> ²	0.925	1.061
<i>R</i> [<i>I</i> > 2 σ (<i>I</i>)]	0.0648	0.0875
<i>wR</i> ₂ (all data)	0.1856	0.1573
Largest diff. peak and hole (eÅ ⁻³)	0.210 and -0.216	0.467 and -0.352
R.M.S deviation from mean (eÅ ⁻³)	0.050	0.043
Code number	9 (CCG_UFAL5)	10 (CCG_UFAL7)

2.2. Cytotoxicity of thiophen-2-thiourea and thiophen-2-iminothiazolidines

The cytotoxicity of the final compounds was evaluated using the MTT assay. Good tolerance was observed for most of the compounds when tested against the *J774* macrophages cell line at a concentration of 10 μ M. Only **4b** presented significant cytotoxicity. The compounds **3b**, **8b** and **8c** showed cell viability (*J774*) above 50 % at 10 μ M (Graphic 1).



Graphic 1. Influence of all synthesized compounds on cell viability after 24 hours of exposure. Each bar represents the mean \pm standard deviation of triplicate experiments (10 and 100 μ M, respectively). Control bars represent cells exposed only to the RPMI-1640 medium and vehicle refers to cells treated with DMSO (0.01%).

2.3. Biological evaluation

The newly synthesized compounds were evaluated by in vitro screening against the amastigote and trypomastigote forms of the *T. cruzi* parasite [25]. A study on cruzain inhibition was carried out using the method described by Ferreira *et al* [26].

2.3.1. Assessment of compound activity against intracellular amastigotes

The amastigote stage was shown to be infective toward phagocytic and non-phagocytic cells, an important process during the cycle in different hosts. The amastigotes multiply by binary fission in the cells of infected tissues. In addition, these evolutionary forms are related to the chronic phase of Chagas disease [27]. The results for activity against the intracellular amastigotes forms are shown in Table 3. Benznidazole (BnZ), with a low IC₅₀ value (1.17 μ M), was used as the positive control. In general, the molecular hybridization strategy can be considered satisfactory, due the cyclization of the compounds increased their potency against the amastigote forms, as observed on comparing **3b** with **4b** and **8b**, and **3c** with **8c**. [28,29].

Furthermore, is possible to observe that the combination of ethyl and allyl groups at R₁ and R₂, respectively, leads to lower activity (IC₅₀ value increases from 6.03 to 9.7 μ M). Therefore, these chemical groups can be considered as unfavorable in relation to activity against these evolutionary forms. Additionally, an *i*-propyl group at R₁ and phenyl group at R₂ seems to be the best combination, increasing the activity, as observed for **3b**, **4b** and **8b**, with IC₅₀ values between 8.78 and

6.03 μM . According to Kryshchysyn *et al.* [6], this is related to the hydrophobicity of the compounds, which leads to an increase in the activity toward evolutionary forms of the *T. cruzi* parasite. However, **8c**, which has an allyl group at R_2 (unfavorable), showed a similar IC_{50} value when compared with **3b**. This fact can be attributed to the presence of a phenyl ring at R_5 in the structure of **8b**, which increases the hydrophobic surface of this compound.

Table 3. Anti-*T. cruzi* activity against intracellular amastigotes for all compounds synthesized.

Code	% Inhibition at 10 μM	IC_{50} Values*
3a	47.0	N.D.
3b	59.64	8.78
3c	11.91	N.D.
3d	37.83	N.D.
4a	20.14	N.D.
4b	39.44	6.96
4c	17.03	N.D.
4d	4.03	N.D.
5c	18.34	N.D.
5d	39.19	N.D.
6a	0.43	N.D.
6c	30.0	N.D.
7a	37.43	N.D.
7b	43.46	N.D.
7c	13.80	N.D.
7d	47.25	N.D.
8a	23.62	N.D.
8b	59.52	6.03
8c	53.07	9.7
8d	36.01	N.D.
<i>BnZ</i> ^a	94.5	1.17
<i>DMSO</i> +medium ^b	1.7	N.D.

*: values in μM ; ^a: Benznidazole, gold-standard drug employed as positive control; ^b: Dimethyl sulfoxide and Roswell Park Memorial Institute (RPMI-1640) medium employed as negative control; N.D.: Not determined.

2.3.2. Activity against *Y* strain trypomastigotes

Intracellular amastigotes transform into trypomastigotes and then burst out of the cell and enter the bloodstream. Trypomastigotes can infect other cells and transform into intracellular amastigotes at new infection sites. The clinical manifestations can result from this infective cycle [27].

All results for anti-*T. cruzi* activity against *Y* strain trypomastigote forms at a concentration of 25 μM are shown in Table 4. Only **4d** showed significant inhibition against these parasite forms and its IC_{50} value was lower than that of *BnZ* (10.3 and 11.4 μM , respectively).

Table 4. Anti-*T. cruzi* activity for all compounds against *Y* strain trypomastigotes.

Code	% Inhibition at 25 μM	IC_{50} Values*
3a	1.6	N.D.
3b	5.8	N.D.
3c	11.9	N.D.
3d	15.1	N.D.
4a	3.2	N.D.
4b	27.0	N.D.
4c	4.5	N.D.
4d	84.1	10.3
5c	7.1	N.D.

5d	6.7	N.D.
6a	9.0	N.D.
6c	16.7	N.D.
7a	6.4	N.D.
7b	6.4	N.D.
7c	5.1	N.D.
7d	7.7	N.D.
8a	5.8	N.D.
8b	4.5	N.D.
8c	5.1	N.D.
8d	6.1	N.D.
<i>BnZ</i> ^a	100	11.4
<i>DMSO</i> + <i>RP</i>	0.01	N.D.
<i>MT</i> ^b		

*: values in μM ; ^a: Benznidazole, gold-standard drug employed as positive control; ^b: Dimethyl sulfoxide and Roswell Park Memorial Institute (RPMI-1640) medium employed as negative control; N.D.: Not determined.

2.3.3. Cruzain inhibition

Cruzain inhibition by thiophen-2-thiourea and thiophen-2-iminothiazolidine derivatives was investigated as a possible mechanism of trypanocidal activity against *T. cruzi* (Table 5). Of the compounds which were most effective against amastigote and trypomastigote forms of *T. cruzi*, **8c** showed the highest potency against cruzain ($\text{IC}_{50} = 2.4 \mu\text{M}$). Additionally, **5c**, **7a**, **7c** and **7d** were also active against the enzyme cruzain, but with moderate potencies. To determine whether the observed activity of the thiophene derivatives **5c**, **7a**, **7c**, **7d** and **8c** was due to nonspecific binding, the assay was repeated in the absence and presence of 0.01 and 0.1% Triton X-100 [30]. Compound **5c** showed a higher cruzain inhibition in the absence of the detergent, possibly indicating aggregation. On the other hand, the level of cruzain inhibition for compounds **7a**, **7c**, **7d** and **8c** did not vary considerably in the presence of the different Triton concentrations, suggesting that the enzyme inhibition is not due to compound aggregation. Additionally, the IC_{50} value for **7c** did not increase in the presence of 2 $\text{mg}\cdot\text{mL}^{-1}$ bovine serum albumin (BSA), with 42 and 50% inhibition of the enzyme at 50 μM in the presence and absence of BSA, respectively. This compound was not sensitive to pre-incubation with BSA, which, at high concentrations competes with the enzyme for colloid particles (aggregates), preventing or reducing enzymatic inhibition due to aggregation [26].

Table 5. Summary of activities for thiophen-2-thiourea and thiophen-2-iminothiazolidine derivatives against the enzyme cruzain.

Code	% Cruzain inhibition at 100 μM ^a			% Cruzain inhibition ^c	
	without pre-incubation	with pre-incubation	IC_{50} , μM ^b	0.01% Triton	0.1% Triton
3a	12 \pm 7	4 \pm 0	N.D.	N.D.	N.D.
3b	43 \pm 4	74 \pm 0.5	N.D.	N.D.	N.D.
3c	29 \pm 3	41 \pm 1	N.D.	N.D.	N.D.
3d	29 \pm 3.6	34 \pm 0.5	N.D.	N.D.	N.D.
4a	0 \pm 0	17 \pm 0.6	N.D.	N.D.	N.D.
4b	33 \pm 8	72 \pm 0.5	N.D.	N.D.	N.D.
4c	23 \pm 8	40 \pm 0.6	N.D.	N.D.	N.D.
4d	45 \pm 2	70 \pm 1	N.D.	N.D.	N.D.

5c	34 ± 6	82 ± 0.5	85 ± 22	33 ± 1 (100 μM)	29 ± 0.6 (100 μM)
5d	38 ± 5 (25μM)	71 ± 0.5 (25μM)	N.D.	N.D.	N.D.
6a	46 ± 2	66 ± 0.8	N.D.	N.D.	N.D.
6c	18 ± 0.5	59 ± 1	N.D.	N.D.	N.D.
7a	66 ± 9	86 ± 0.5	121 ± 34	5.4 ± 3 (100 μM)	18 ± 4 (100 μM)
7b	32 ± 9	77 ± 1	N.D.	N.D.	N.D.
7c	64 ± 7	89 ± 0.4	50 ± 10	47 ± 2.5 (50 μM)	44 ± 0.4 (50 μM)
7d	52 ± 15	80 ± 0.7	111 ± 9	53 ± 6.2 (100 μM)	52.7 ± 0.4 (100 μM)
8a	16 ± 2 (50μM)	40 ± 0.5 (50μM)	N.D.	N.D.	N.D.
8b	13 ± 4	25 ± 1	N.D.	N.D.	N.D.
8c	87 ± 5	97 ± 0.3	2.4 ± 1.2	62 ± 3.2 (6.25 μM)	55 ± 1.3 (6.25 μM)
8d	29 ± 4	67 ± 0.5	N.D.	N.D.	N.D.
<i>E-64^d</i>	100 ± 0	100 ± 0	0.4	N.D.	N.D.

^a: The results represent the average and standard error of two independent experiments in triplicate. Errors are given as the ratio between the standard deviation and the square root of the number of measurements; ^b: IC₅₀ values represent the average and standard error of two independent experiments which were determined based on at least 9 compound concentrations in triplicate; ^c: The compounds were tested at concentrations close to the IC₅₀; ^d: Potent inhibitor employed as positive control; N.D.: Not determined.

2.3.4. Molecular docking studies

Since 2008, computational methodologies such as molecular docking and high-throughput screening (HTS) have been employed to providing new scaffolds with high potency and good tolerance [8]. Molecular docking models have been shown to adequately predict the binding mode associated with the binding of different anti-*T. cruzi* compounds to cruzain [4]. Therefore, in order to gain a better insight into the nature of the trypanocidal activity displayed by the novel thiophen-2-iminothiazolidine reported herein, molecular docking studies were performed with cruzain. The most active compound (**8c**) against amastigote forms and the enzyme cruzain provided a negative values for the theoretical energy binding ($E_b = -7.39$ kcal·mol⁻¹). This indicates interaction (via dipole-dipole) between the hybridized sulfur sp³ atom at the thiazolidine ring and Gly66 (Fig. 7) [5,29]. According to Martinez-Moyaorga *et al.*[8], this amino acid is the main key residue related to anti-*T. cruzi* activity, and interactions with water molecules are not associated with inhibitory activity.

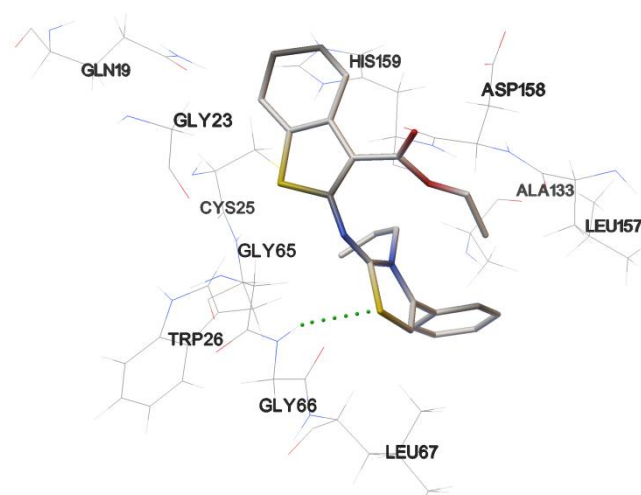


Figure 7. **8c** in complex with enzyme cruzain. Green dots represent dipole-dipole interaction between hybridized sulfur sp³ atom at thiazolidine ring and Gly 66.

Normally, in a complex of hydrophobic compounds with the enzyme cruzain, a phenyl ring (when present) is allocated to the S2 subsite pocket and this is observed to be related to an increase the binding affinity [8]. Based on this, the cruzain subsite analysis shows that compound **8c** can interact with subsites S1 and S2 simultaneously. For this compound, the phenyl ring is allocated to S2 (high hydrophobicity) and the tetrahydrobenzothiophene bicycle is allocated to S1 (low hydrophobicity) (Fig. 8). In addition, docking results showed that the compounds **5c**, **7a**, **7c** and **7d** does not provided satisfactory E_b values in comparison with **8c**, and are not able to interact with Gly66 amino acid.

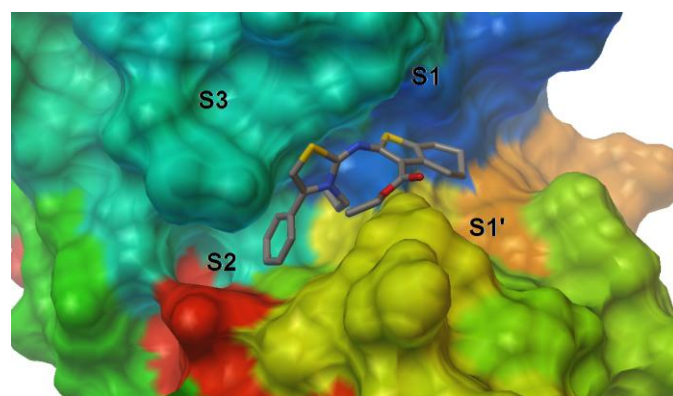


Figure 8. Cruzain binding site showing the subsites S1', S1, S2 and S3. **8c** allocated to S2 and S1 subsites.

3. Conclusion

In this study new thiazolidine based conjugates with the thiophene moiety in position 2 are described using accessible methods. The assay to determine the trypanocidal activity of synthesized compounds allowed us to identify thiophene-thiourea hybrid **3b** and thiophene-thiazolidine hybrids **4b**, **8b** and **8c**, which were found to be the most active derivatives against amastigote form, with significant IC₅₀ values between 9.7 and 6.03 μM. In addition, **8c** showed excellent ability to inhibit the cruzain enzyme, with an IC₅₀ value of 2.4 μM. The results of the *in silico* studies corroborated the *in vitro* cruzain inhibition, showing that the most stable molecule is also the most potent cruzain inhibitor. Modifications to improve the potency of the

most potent derivatives are currently under progress in our

4. Experimental section

4.1. Chemistry

All reagents were commercial grade and purified according to the established procedures. Melting points (m.p.) were detected with open capillaries using MSTecnon® PFMII Digital Melting point, and are incorrect. NMR analyses were performed on Bruker® Avance DRX 400 MHz Spectrometer by using tetramethylsilane (TMS) as internal standard. The chemical shifts were reported in δ units, and coupling constants (J) were measured in hertz. The peaks are presented as *s* (singlet), *d* (doublet), *t* (triplet), *q* (quartet), *qi* (quintet), *sex* (sextet), *sep* (septet), *br s* (broad singlet), *dd* (double doublet), *ddt* (double doublet of triplet), *m* (multiplet). The reactions were monitored by TLC (Merck®, silica gel, type 60, 0.25 mm).

4.1.1. Procedure for Synthesis of 2-aminothiophene (1,2)

A mixture of cyclohexanone (1 mmol), an activated nitrile (1 eq.), morpholine (1 eq.) and elemental sulfur (1 eq.) in 5 ml of ethanol was stirred at 0 °C overnight. After, the solvent was evaporated at reduced pressure and the crude product was extracted with ethyl acetate thrice. The organic layer was treated with anhydrous sodium sulphate and evaporated again. Finally the final compounds were purified by recrystallization from MeOH/water.

4.1.1.1. Ethyl 2-amino-4,5,6,7-tetrahydrobenzo[b]thiophene-3-carboxylate (1)

Yellow crystalline solid. Yield: 98%, m.p. 134-135 °C. ¹H NMR (400 MHz, DMSO-*d*₆) δ 1.20 (3H, *t*, J = 7.1, CH₃), 1.60-1.65 (4H, *m*, CH₂), 2.35-2.37 (2H, *m*, CH₂), 2.55-2.56 (2H, *m*, CH₂), 4.11 (2H, *q*, J = 7.3, CH₂CH₃), 7.14 (2H, *br s*, NH). ¹³C NMR (100 MHz, DMSO-*d*₆) δ 14.18 (CH₃), 22.34 (CH₂), 22.76 (CH₂), 23.88 (CH₂), 26.49 (CH₂), 58.71 (OCH₂), 103.16 (Cq), 115.96 (Cq), 131.50 (Cq), 163.19 (Cq), 165.32 (C=O).

4.1.1.2. Isopropyl 2-amino-4,5,6,7-tetrahydrobenzo[b]thiophene-3-carboxylate (2)

Yellow amorphous solid. Yield: 70%, m.p. 67-68 °C. ¹H NMR (400 MHz, DMSO-*d*₆) δ 1.20 (6H, *d*, J = 6.2, CH₃), 1.60-1.65 (4H, *m*, CH₂), 2.35-2.38 (2H, *m*, CH₂), 2.53-2.55 (2H, *m*, CH₂), 4.96 (1H, *sep*, J = 6.2, CH), 7.11 (2H, *br s*, NH). ¹³C NMR (100 MHz, DMSO-*d*₆) δ 22.32 (CH₃), 22.83 (CH₂), 23.17 (CH₂), 24.30 (CH₂), 27.01 (CH₂), 66.43 (CH), 103.43 (Cq), 116.16 (Cq), 131.85 (Cq), 162.78 (Cq), 165.21 (C=O).

4.1.2. Procedure for Synthesis of intermediates Thiophen-2-thiourea (3a-d)

A mixture of 2-aminothiophene (1 mmol) and isothiocyanate (1.1 eq) in 15 ml ethanol was stirred until reflux overnight. After, the solvent was evaporated at reduced pressure and the crude product was extracted with ethyl acetate thrice. The organic layer was treated with anhydrous sodium sulphate and evaporated again. Subsequently, was performed a flash chromatography using hexane/ethyl acetate (8:2) as eluent. Finally, the product was recrystallized from MeOH/water.

4.1.2.1. Ethyl 2-(3-phenylthioureido)-4,5,6,7-tetrahydrobenzo[b]thiophene-3-carboxylate (3a)

White amorphous solid. Yield: 98%, m.p. 199-200 °C. ¹H NMR (400 MHz, CDCl₃) δ 1.25 (3H, *t*, J = 7.1, CH₃), 1.74-1.79 (4H, *m*, CH₂), 2.63-2.66 (2H, *m*, CH₂), 2.71-2.74 (2H, *m*, CH₂),

laboratory.

4.13 (2H, *q*, J = 7.1, CH₂CH₃), 7.33-7.39 (3H, *m*, ArH), 7.46-7.50 (2H, *m*, ArH), 7.98 (1H, *br s*, NH), 12.17 (1H, *br s*, NH). ¹³C NMR (100 MHz, CDCl₃) δ 14.19 (CH₃), 22.86 (CH₂), 22.97 (CH₂), 24.32 (CH₂), 26.31 (CH₂), 60.39 (OCH₂), 113.12 (Cq), 125.62 (CH Ar), 126.86 (Cq), 127.74 (CH Ar), 130.01 (CH Ar), 130.89 (Cq), 135.87 (Cq Ar), 149.78 (Cq), 166.31 (C=O), 176.17 (C=S).

4.1.2.2. Isopropyl 2-(3-phenylthioureido)-4,5,6,7-tetrahydrobenzo[b]thiophene-3-carboxylate (3b)

Pale brown amorphous solid. Yield: 60%, m.p. 194-195 °C. ¹H NMR (400 MHz, CDCl₃) δ 1.24 (6H, *d*, J = 6.2, CH₃), 1.74-1.79 (4H, *m*, CH₂), 2.63-2.65 (2H, *m*, CH₂), 2.71-2.73 (2H, *m*, CH₂), 5.01 (1H, *sep*, J = 6.2, CH), 7.33-7.38 (3H, *m*, ArH), 7.45-7.49 (2H, *m*, ArH), 7.92 (1H, *br s*, NH), 12.30 (1H, *br s*, NH). ¹³C NMR (100 MHz, CDCl₃) δ 21.89 (CH₃), 22.91 (CH₂), 22.97 (CH₂), 24.34 (CH₂), 26.42 (CH₂), 68.09 (CH), 113.43 (Cq), 125.50 (CH Ar), 126.84 (Cq), 127.62 (CH Ar), 129.95 (CH Ar), 130.79 (Cq), 135.94 (Cq Ar), 149.77 (Cq), 166.09 (C=O), 176.19 (C=S).

4.1.2.3. Ethyl 2-(3-allylthioureido)-4,5,6,7-tetrahydrobenzo[b]thiophene-3-carboxylate (3c)

Pale brown amorphous solid. Yield: 80%, m.p. 173-174 °C. ¹H NMR (400 MHz, CDCl₃) δ 1.38 (3H, *t*, J = 7.1, CH₃), 1.76-1.81 (4H, *m*, CH₂), 2.62-2.65 (2H, *m*, CH₂), 2.75-2.77 (2H, *m*, CH₂), 4.13-4.18 (2H, *m*, CH₂CH=CH₂), 4.32 (2H, *q*, J = 7.1, CH₂CH₃), 5.26 (1H, *dd*, J = 0.9 and 10.2, CH₂CH=CH₂), 5.36 (1H, *d*, J = 17.1, CH₂CH=CH₂), 5.92 (1H, *ddt*, J = 5.8, 10.2 and 17.1, CH₂CH=CH₂), 6.34 (1H, *br s*, NH), 12.14 (1H, *br s*, NH). ¹³C NMR (100 MHz, CDCl₃) δ 14.28 (CH₃), 22.88 (CH₂), 22.98 (CH₂), 24.31 (CH₂), 26.37 (CH₂), 46.62 (CH₂CH=CH₂), 60.66 (OCH₂), 112.03 (Cq), 118.22 (CH₂CH=CH₂), 126.26 (Cq), 130.52 (Cq), 131.90 (CH₂CH=CH₂), 151.04 (Cq), 167.44 (C=O), 176.93 (C=S).

4.1.2.4. Isopropyl 2-(3-allylthioureido)-4,5,6,7-tetrahydrobenzo[b]thiophene-3-carboxylate (3d)

Pale brown amorphous solid. Yield: 80%, m.p. 140-141 °C. ¹H NMR (400 MHz, CDCl₃) δ 1.36 (6H, *t*, J = 6.3, CH₃), 1.77-1.79 (4H, *m*, CH₂), 2.62-2.64 (2H, *m*, CH₂), 2.74-2.77 (2H, *m*, CH₂), 4.12-4.18 (2H, *m*, CH₂CH=CH₂), 5.19 (1H, *sep*, J = 6.3, CH), 5.26 (1H, *dd*, J = 1.0 and 10.2, CH₂CH=CH₂), 5.36 (1H, *d*, J = 17.1, CH₂CH=CH₂), 5.92 (1H, *ddt*, J = 5.8, 10.2 and 17.1, CH₂CH=CH₂), 6.28 (1H, *br s*, NH), 12.19 (1H, *br s*, NH). ¹³C NMR (100 MHz, CDCl₃) δ 22.06 (CH₃), 22.96-23.01 (CH₂), 24.35 (CH₂), 26.51 (CH₂), 46.64 (CH₂CH=CH₂), 68.37 (CH), 112.38 (Cq), 118.22 (CH₂CH=CH₂), 126.28 (Cq), 130.56 (CH₂CH=CH₂), 132.00 (Cq), 150.88 (Cq), 166.99 (C=O), 176.97 (C=S).

4.1.3. Procedure for Synthesis of Thiophen-2-thiazolidine (4a-d, 5c,d, 6a, 6c, 7a-d and 8a-d)

A mixture of thiophen-2-thiourea (1 mmol) and the respectively dielectrophile (1.0 eq) in 15 ml ethanol (for synthesis of 7a-d was utilized toluene) was stirred until reflux overnight. After, the solvent was evaporated at reduced pressure and the crude product was extracted with ethyl acetate thrice. The organic layer was treated with anhydrous sodium sulphate and evaporated again. Finally the final compounds were purified by flash chromatography using hexane/ethyl acetate (8:2) as eluent.

4.1.3.1. (Z)-Ethyl 2-((4-oxo-3-phenylthiazolidin-2-ylidene)amino)-4,5,6,7-tetrahydrobenzo[b]thiophene-3-carboxylate (**4a**)

White amorphous solid. Yield: 95%, m.p. 195-196 °C. ¹H NMR (400 MHz, CDCl₃) δ 1.31 (3H, t, J = 7.1, CH₃), 1.79-1.91 (4H, m, CH₂), 2.75-2.78 (2H, m, CH₂), 2.93-2.96 (2H, m, CH₂), 3.85 (2H, s, SCH₂), 4.22 (2H, q, J = 7.1, CH₂CH₃), 7.32-7.35 (2H, m, ArH), 7.54-7.56 (3H, m, ArH). ¹³C NMR (100 MHz, CDCl₃) δ 14.27 (CH₃), 22.27 (CH₂), 22.98 (CH₂), 25.11 (CH₂), 25.35 (CH₂), 34.97 (SCH₂), 61.88 (CH₂CH₃), 119.31 (Cq), 129.10 (CH Ar), 129.83 (CH Ar), 130.12 (CH Ar), 131.71 (Cq), 131.98 (Cq), 135.50 (Cq Ar), 155.66 (Cq), 158.49 (C=N), 161.99 (NC=O), 168.48 (C=O).

4.1.3.2. (Z)-Isopropyl 2-((4-oxo-3-phenylthiazolidin-2-ylidene)amino)-4,5,6,7-tetrahydrobenzo[b]thiophene-3-carboxylate (**4b**)

Dark yellow oil. Yield: 60%. ¹H NMR (400 MHz, CDCl₃) δ 1.20 (6H, d, J = 6.0, CH₃), 1.80-1.89 (4H, m, CH₂), 2.60-2.68 (2H, m, CH₂), 2.76-2.93 (2H, m, CH₂), 3.84 (2H, s, SCH₂), 5.85 (1H, sep, J = 6.2, CH), 7.30-7.32 (2H, m, ArH), 7.50-7.56 (3H, m, ArH). ¹³C NMR (100 MHz, CDCl₃) δ 22.00 (CH₃), 22.27 (CH₂), 22.98 (CH₂), 25.11 (CH₂), 25.35 (CH₂), 34.66 (SCH₂), 61.61 (CH), 119.33 (Cq), 129.11 (CH Ar), 129.83 (CH Ar), 130.13 (CH Ar), 131.72 (Cq), 132.01 (Cq), 135.46 (Cq Ar), 155.49 (Cq), 158.46 (C=N), 161.99 (NC=O), 168.95 (C=O).

4.1.3.3. (Z)-Ethyl 2-((3-allyl-4-oxothiazolidin-2-ylidene)amino)-4,5,6,7-tetrahydrobenzo[b]thiophene-3-carboxylate (**4c**)

Pale orange amorphous solid. Yield: 68%, m.p. 94-95 °C. ¹H NMR (400 MHz, CDCl₃) δ 1.29 (3H, t, J = 7.1, CH₃), 1.75-1.86 (4H, m, CH₂), 2.67 (2H, t, J = 6.0, CH₂), 2.76 (2H, t, J = 6.1, CH₂), 3.90 (2H, s, SCH₂), 4.24 (2H, q, J = 7.1, CH₂CH₃), 4.46 (2H, d, J = 6.0, CH₂CH=CH₂), 5.24 (1H, d, J = 10.1, CH₂CH=CH₂), 5.34 (1H, d, J = 17.1, CH₂CH=CH₂), 5.95 (1H, ddt, J = 6.1, 10.1 and 16.9, CH₂CH=CH₂). ¹³C NMR (100 MHz, CDCl₃) δ 14.44 (CH₃), 22.61 (CH₂), 23.02 (CH₂), 25.0 (CH₂), 26.18 (CH₂), 33.39 (SCH₂), 45.50 (CH₂CH=CH₂), 60.04 (OCH₂), 119.06 (CH₂CH=CH₂), 120.12 (Cq), 129.52 (Cq), 130.55 (CH₂CH=CH₂), 134.50 (Cq), 151.82 (Cq), 155.86 (C=N), 163.60 (NC=O), 171.00 (C=O).

4.1.3.4. (Z)-Isopropyl 2-((3-allyl-4-oxothiazolidin-2-ylidene)amino)-4,5,6,7-tetrahydrobenzo[b]thiophene-3-carboxylate (**4d**)

Pale yellow amorphous solid. Yield: 55%, m.p. 133-134 °C. ¹H NMR (400 MHz, CDCl₃) δ 1.04 (6H, d, J = 6.2, CH₃), 1.53-1.61 (4H, m, CH₂), 2.42-2.45 (2H, m, CH₂), 2.50-2.53 (2H, m, CH₂), 3.66 (2H, s, SCH₂), 4.23 (2H, d, J = 6.02, CH₂CH=CH₂), 4.91 (1H, sep, J = 6.25, CH), 5.01 (1H, dd, J = 1.2 and 10.1, CH₂CH=CH₂), 5.12 (1H, dd, J = 1.2 and 17.1, CH₂CH=CH₂), 5.71 (1H, ddt, J = 6.1, 10.1 and 16.2, CH₂CH=CH₂). ¹³C NMR (100 MHz, CDCl₃) δ 22.27 (CH₃), 22.87 (CH₂), 23.25 (CH₂), 25.22 (CH₂), 26.44 (CH₂), 33.52 (SCH₂), 45.72 (CH₂CH=CH₂), 67.54 (CH), 119.40 (CH₂CH=CH₂), 120.61 (Cq), 129.73 (Cq), 130.83 (CH₂CH=CH₂), 134.60 (Cq), 151.88 (Cq), 156.17 (C=N), 163.17 (NC=O), 171.19 (C=O).

4.1.3.5. (Z)-Ethyl 3-allyl-2-((3-(ethoxycarbonyl)-4,5,6,7-tetrahydrobenzo[b]thiophen-2-yl)imino)-4-methyl-2,3-dihydrothiazole-5-carboxylate (**5c**)

Pale orange amorphous solid. Yield: 40%, m.p. 60-61 °C. ¹H NMR (400 MHz, CDCl₃) δ 1.29 (3H, t, J = 7.1, CH₃), 1.31 (3H, t,

J = 7.1, CH₃), 1.74-1.82 (4H, m, CH₂), 2.57 (3H, s, CH₃), 2.65-2.68 (2H, m, CH₂), 2.74-2.77 (2H, m, CH₂), 4.24 (2H, q, J = 7.1, CH₂), 4.25 (2H, q, J = 7.1, CH₂), 4.69 (2H, d, J = 5.2, CH₂CH=CH₂), 5.15 (1H, dd, J = 0.8 and 17.1, CH₂CH=CH₂), 5.21 (1H, dd, J = 0.9 and 10.3, CH₂CH=CH₂), 5.94 (1H, ddt, J = 5.2, 10.4 and 15.6, CH₂CH=CH₂). ¹³C NMR (100 MHz, CDCl₃) δ 12.85 (CH₃), 14.37 (CH₃), 14.47 (CH₃), 22.80 (CH₂), 23.17 (CH₂), 25.20 (CH₂), 26.32 (CH₂), 47.13 (CH₂CH=CH₂), 59.74 (CH₂CH₃), 60.96 (CH₂CH₃), 102.46 (C=C), 117.65 (CH₂CH=CH₂), 118.92 (Cq), 127.25 (Cq), 131.44 (CH₂CH=CH₂), 134.24 (Cq), 146.29 (C=C), 153.96 (Cq), 156.71 (C=N), 161.72 (C=O), 164.28 (C=O).

4.1.3.6. (Z)-Ethyl 3-allyl-2-((3-(isopropoxycarbonyl)-4,5,6,7-tetrahydrobenzo[b]thiophen-2-yl)imino)-4-methyl-2,3-dihydrothiazole-5-carboxylate (**5d**)

Dark brown oil. Yield: 75%. ¹H NMR (400 MHz, CDCl₃) δ 1.29 (6H, d, J = 6.2, CH₃), 1.33 (3H, t, J = 7.16, CH₂CH₃), 1.77-1.84 (4H, m, CH₂), 2.60 (3H, s, CH₃), 2.63-2.69 (2H, m, CH₂), 2.71-2.77 (2H, m, CH₂), 4.27 (2H, q, J = 7.12, CH₂CH₃), 4.71-4.72 (2H, m, CH₂CH=CH₂), 5.18 (1H, sep, J = 6.2, CH), 5.20 (1H, dd, J = 1.2 and 10.1, CH₂CH=CH₂), 5.94 (1H, ddt, J = 6.2, 10.1 and 17.0, CH₂CH=CH₂). ¹³C NMR (100 MHz, CDCl₃) δ 12.90 (CH₃), 14.39 (CH₃), 22.13 (CH₃), 22.86 (CH₂), 23.21 (CH₂), 25.22 (CH₂), 26.35 (CH₂), 47.05 (CH₂CH=CH₂), 60.95 (CH₂CH₃), 102.20 (C=C), 119.18 (Cq), 127.13 (Cq), 131.55 (CH₂CH=CH₂), 134.07 (Cq), 146.29 (C=C), 154.03 (Cq), 156.36 (C=N), 161.87 (C=O), 163.94 (C=O).

4.1.3.7. (Z)-Ethyl 2-((3-(ethoxycarbonyl)-4,5,6,7-tetrahydrobenzo[b]thiophen-2-yl)imino)-4-oxo-3-phenylthiazolidine-5-carboxylate (**6a**)

Pale orange amorphous solid. Yield: 60%, m.p. 130-131 °C. ¹H NMR (400 MHz, CDCl₃) δ 1.30 (6H, t, J = 7.1, CH₃), 1.80-1.89 (4H, m, CH₂), 2.75-2.78 (2H, m, CH₂), 2.92-2.95 (2H, m, CH₂), 4.25 (4H, q, J = 7.0, CH₂CH₃), 5.28 (1H, SCH), 7.33-7.34 (2H, m, CH Ar), 7.35-7.54 (3H, m, CH Ar). ¹³C NMR (100 MHz, CDCl₃) δ 14.05 (CH₃), 22.24 (CH₂), 22.96 (CH₂), 25.11 (CH₂), 25.32 (CH₂), 54.00 (SCH), 62.87 (CH₂CH₃), 119.51 (Cq), 129.10 (CH Ar), 129.97 (CH Ar), 130.33 (CH Ar), 130.94 (Cq), 131.17 (Cq), 132.32 (Cq), 135.05 (Cq Ar), 154.48 (C=N), 158.32 (NC=O), 161.59 (C=O), 165.49 (C=O).

4.1.3.8. (Z)-Ethyl 3-allyl-2-((3-(ethoxycarbonyl)-4,5,6,7-tetrahydrobenzo[b]thiophen-2-yl)imino)-4-oxothiazolidine-5-carboxylate (**6c**)

Pale orange amorphous solid. Yield: 50%, m.p. 80-81 °C. ¹H NMR (400 MHz, CDCl₃) δ 1.30 (6H, t, J = 7.2, CH₃), 1.77-1.84 (4H, m, CH₂), 2.67-2.70 (2H, m, CH₂), 2.77-2.80 (2H, m, CH₂), 4.27 (4H, q, J = 7.2, CH₂), 4.54 (2H, d, J = 6.0, CH₂CH=CH₂), 4.98 (1H, dd, J = 1.6 and 17.0, CH₂CH=CH₂), 5.13 (1H, dd, J = 1.2 and 10.4, CH₂CH=CH₂), 5.96 (1H, ddt, J = 5.1, 10.2 and 17.1, CH₂CH=CH₂), 6.08 (1H, s, SCH). ¹³C NMR (100 MHz, CDCl₃) δ 14.59 (CH₃), 14.69 (CH₃), 23.04 (CH₂), 23.42 (CH₂), 25.44 (CH₂), 26.54 (CH₂), 47.31 (CH₂CH=CH₂), 59.94 (SCH), 61.16 (CH₂CH₃), 117.87 (CH₂CH=CH₂), 119.05 (Cq), 127.34 (Cq), 131.72 (CH₂CH=CH₂), 134.46 (Cq), 146.47 (Cq), 154.46 (Cq), 156.77 (C=N), 161.99 (NC=O), 164.54 (C=O), 166.11 (C=O).

4.1.3.9. (Z)-2-((3-(Ethoxycarbonyl)-4,5,6,7-tetrahydrobenzo[b]thiophen-2-yl)imino)-4-oxo-3-phenylthiazolidine-5-yl)acetic acid (**7a**)

Red amorphous solid. Yield: 80%, m.p. 99-100 °C. ¹H NMR (400 MHz, CDCl₃) δ 1.24 (3H, t, J = 7.4, CH₃), 1.74-1.81 (4H, m, CH₂), 2.61-2.65 (2H, m, CH₂), 2.69-2.74 (2H, m, CH₂), 3.10 (1H,

dd, $J = 8.9, 17.6$ (CHa), 3.35 (1H, *dd*, $J = 3.2, 17.6$, CHb), 4.17 (2H, *q*, $J = 7.4$), 4.53 (1H, *dd*, $J = 3.2, 8.9$, SCH), 7.38-7.43 (3H, *m*, ArH), 7.49-7.53 (2H, *m*, ArH). ^{13}C NMR (100 MHz, CDCl_3) δ 14.40 (CH_3), 22.58 (CH_2), 22.97 (CH_2), 24.95 (CH_2), 26.23 (CH_2), 26.30 (CH_2), 37.50 (CH_2CO), 43.86 (SCH), 60.24 (CH_2CH_3), 119.33 (Cq), 127.92 (CH Ar), 129.11 (CH Ar), 129.26 (CH Ar), 129.55 (Cq), 134.28 (Cq Ar), 134.40 (Cq), 152.66 (Cq), 157.07 (C=N), 163.72 (NC=O), 173.03 (C=O), 174.13 (C=O).

4.1.3.10. (Z)-2-(2-((3-(Isopropoxycarbonyl)-4,5,6,7-tetrahydrobenzo[b]thiophen-2-yl)imino)-4-oxo-3-phenyl-thiazolidin-5-yl)acetic acid (**7b**)

Dark orange oil. Yield: 70%. ^1H NMR (400 MHz, CDCl_3) δ 1.22 (6H, *d*, $J = 6.3$, CH_3), 1.74-1.80 (4H, *m*, CH_2), 2.61-2.62 (2H, *m*, CH_2), 2.69-2.72 (2H, *m*, CH_2), 3.08 (1H, *dd*, $J = 9.2, 17.9$, CHa), 3.34 (1H, *dd*, $J = 3.5, 17.9$, CHb), 4.52 (1H, *dd*, $J = 3.5, 9.2$, SCH), 5.09 (1H, *sep*, $J = 6.3$, CH), 7.38-7.44 (3H, *m*, ArH), 7.47-7.51 (2H, *m*, ArH). ^{13}C NMR (100 MHz, CDCl_3) δ 22.02 (CH_3), 22.05 (CH_3), 22.63 (CH_2), 22.98 (CH_2), 24.94 (CH_2), 26.30 (CH_2), 37.64 (CH_2CO), 43.81 (SCH), 67.49 (CH), 119.43 (Cq), 127.89 (CH Ar), 129.01 (CH Ar), 129.21 (CH Ar), 129.34 (Cq), 134.25 (Cq Ar), 134.27 (Cq), 152.70 (Cq), 157.01 (C=N), 163.14 (NC=O), 173.05 (C=O), 173.80 (C=O).

4.1.3.11. (Z)-2-(3-Allyl-2-((3-(ethoxycarbonyl)-4,5,6,7-tetrahydrobenzo[b]thiophen-2-yl)imino)-4-oxothiazolidin-5-yl)acetic acid (**7c**)

Dark red oil. Yield: 86%. ^1H NMR (400 MHz, CDCl_3) δ 1.29 (3H, *t*, $J = 7.1$, CH_3), 1.78-1.80 (4H, *m*, CH_2), 2.64-2.65 (2H, *m*, CH_2), 2.72-2.75 (2H, *m*, CH_2), 2.91 (1H, *dd*, $J = 9.8, 17.9$, CHa), 3.33 (1H, *dd*, $J = 3.5, 17.9$, CHb), 4.24 (2H, *q*, $J = 7.1$, CH_2), 4.39 (1H, *dd*, $J = 3.5, 9.8$, SCH), 4.45 (2H, *d*, $J = 5.8$, $\text{CH}_2\text{CH}=\text{CH}_2$), 5.23 (1H, *d*, $J = 10.2$, $\text{CH}_2\text{CH}=\text{CH}_2$), 5.33 (1H, *d*, $J = 17.1$, $\text{CH}_2\text{CH}=\text{CH}_2$), 5.93 (1H, *ddt*, $J = 6.1, 10.1$ and 16.9 , $\text{CH}_2\text{CH}=\text{CH}_2$). ^{13}C NMR (100 MHz, CDCl_3) δ 14.44 (CH_3), 22.60 (CH_2), 23.01 (CH_2), 25.01 (CH_2), 26.18 (CH_2), 37.53 (CH_2CO), 44.01 (SCH), 45.61 ($\text{CH}_2\text{CH}=\text{CH}_2$), 60.18 (OCH₂), 119.01 ($\text{CH}_2\text{CH}=\text{CH}_2$), 120.26 (Cq), 129.72 (Cq), 130.42 ($\text{CH}_2\text{CH}=\text{CH}_2$), 134.49 (Cq), 151.75 (Cq), 154.85 (C=N), 163.71 (NC=O), 174.51 (C=O), 174.60 (C=O).

4.1.3.12. (Z)-2-(3-Allyl-2-((3-(isopropoxycarbonyl)-4,5,6,7-tetrahydrobenzo[b]thiophen-2-yl)imino)-4-oxothiazolidin-5-yl)acetic acid (**7d**)

Pale orange amorphous solid. Yield: 90%, m.p. 139-140 °C. ^1H NMR (400 MHz, CDCl_3) δ 1.28 (6H, *dd*, $J = 2.0$ and 6.3 , CH_3), 1.76-1.83 (4H, *m*, CH_2), 2.64-2.67 (2H, *m*, CH_2), 2.72-2.75 (2H, *m*, CH_2), 2.90 (1H, *dd*, $J = 9.9, 17.9$, CHa), 3.34 (1H, *dd*, $J = 3.5, 17.9$, CHb), 4.40 (1H, *dd*, $J = 3.5, 9.9$, SCH), 4.46 (2H, *d*, $J = 5.9$, $\text{CH}_2\text{CH}=\text{CH}_2$), 5.14 (1H, *sep*, $J = 6.3$, CH), 5.24 (1H, *dd*, $J = 1.0$ and 10.2 , $\text{CH}_2\text{CH}=\text{CH}_2$), 5.34 (1H, *dd*, $J = 1.24$ and 17.1 , $\text{CH}_2\text{CH}=\text{CH}_2$), 5.93 (1H, *ddt*, $J = 6.1, 10.1$ and 16.3 , $\text{CH}_2\text{CH}=\text{CH}_2$). ^{13}C NMR (100 MHz, CDCl_3) δ 22.05 (CH_3), 22.08 (CH_3), 22.63 (CH_2), 23.01 (CH_2), 25.00 (CH_2), 26.20 (CH_2), 37.57 (CH_2CO), 43.98 (SCH), 45.57 ($\text{CH}_2\text{CH}=\text{CH}_2$), 67.55 (CH), 119.21 ($\text{CH}_2\text{CH}=\text{CH}_2$), 120.60 (Cq), 129.74 (Cq), 130.44 ($\text{CH}_2\text{CH}=\text{CH}_2$), 134.29 (Cq), 151.54 (Cq), 154.80 (C=N), 163.28 (NC=O), 172.63 (C=O), 174.70 (C=O).

4.1.3.13. (Z)-Ethyl 2-((3,4-diphenylthiazol-2(3H)-ylidene)amino)-4,5,6,7-tetrahydrobenzo[b]thiophene-3-carboxylate (**8a**)

Pale yellow amorphous solid. Yield: 65%, m.p. 120-121 °C. ^1H NMR (400 MHz, CDCl_3) δ 1.17 (3H, *t*, $J = 7.2$, CH_3), 1.75-

1.84 (4H, *m*, CH_2), 2.65-2.68 (2H, *m*, CH_2), 2.73-2.76 (2H, *m*, CH_2), 4.14 (2H, *q*, $J = 7.2$, CH_2), 6.22 (1H, *s*, SCH), 7.07-7.25 (7H, *m*, CH Ar), 7.30-7.36 (3H, *m*, CH Ar). ^{13}C NMR (100 MHz, CDCl_3) δ 14.33 (CH_3), 22.69 (CH_2), 23.08 (CH_2), 25.06 (CH_2), 26.28 (CH_2), 59.34 (CH_2CH_3), 100.49 (SCH), 117.99 (Cq), 128.38 (CH Ar), 128.45 (CH Ar), 128.54 (CH Ar), 128.60 (CH Ar), 128.73 (CH Ar), 128.85 (CH Ar), 128.93 (CH Ar), 128.99 (CH Ar), 129.10 (CH Ar), 129.32 (CH Ar), 130.11 (Cq), 134.19 (Cq), 140.42 (Cq Ar), 164.50 (C=O).

4.1.3.14. (Z)-Isopropyl 2-((3,4-diphenylthiazol-2(3H)-ylidene)amino)-4,5,6,7-tetrahydrobenzo[b]thiophene-3-carboxylate (**8b**)

Yellow crystalline solid. Yield: 80%, m.p. 140-141 °C. ^1H NMR (400 MHz, CDCl_3) δ 1.19 (6H, *d*, $J = 6.2$, CH_3), 1.76-1.82 (4H, *m*, CH_2), 2.63-2.66 (2H, *m*, CH_2), 2.72-2.75 (2H, *m*, CH_2), 5.09 (1H, *sep*, $J = 6.2$, CH), 6.23 (1H, *s*, SCH), 7.07-7.09 (2H, *m*, CH Ar), 7.18-7.34 (8H, *m*, CH Ar). ^{13}C NMR (100 MHz, CDCl_3) δ 21.97 (CH_3), 22.80 (CH_2), 23.16 (CH_2), 25.05 (CH_2), 26.33 (CH_2), 67.01 (CH), 99.46 (SCH), 117.84 (Cq), 126.86 (Cq), 127.95 (CH Ar), 128.31 (CH Ar), 128.38 (CH Ar), 128.62 (CH Ar), 128.64 (CH Ar), 128.90 (CH Ar), 131.01 (Cq), 134.14 (Cq), 137.00 (Cq Ar), 139.98 (Cq Ar), 152.36 (Cq), 161.67 (Cq), 163.81 (C=O).

4.1.3.15. (Z)-Ethyl 2-((3-allyl-4-phenylthiazol-2(3H)-ylidene)amino)-4,5,6,7-tetrahydrobenzo[b]thiophene-3-carboxylate (**8c**)

Green oil. Yield: 78%. ^1H NMR (400 MHz, CDCl_3) δ 1.30 (3H, *t*, $J = 7.1$, CH_3), 1.75-1.86 (4H, *m*, CH_2), 2.69 (2H, *t*, $J = 6.0$, CH_2), 2.78 (2H, *t*, $J = 6.0$, CH_2), 4.26 (2H, *q*, $J = 7.1$, CH_2CH_3), 4.54 (2H, *d*, $J = 4.8$, $\text{CH}_2\text{CH}=\text{CH}_2$), 4.98 (1H, *dd*, $J = 10.3$ and 17.2 , $\text{CH}_2\text{CH}=\text{CH}_2$), 5.13 (1H, *dd*, $J = 10.3$ and $J = 17.1$, $\text{CH}_2\text{CH}=\text{CH}_2$), 5.95 (1H, *ddt*, $J = 5.2, 10.3$ and 17.1 , $\text{CH}_2\text{CH}=\text{CH}_2$), 6.08 (1H, *s*, SCH), 7.37-7.40 (2H, *m*, Ar H), 7.43-7.45 (3H, *m*, Ar H). ^{13}C NMR (100 MHz, CDCl_3) δ 14.44 (CH_3), 22.87 (CH_2), 23.22 (CH_2), 25.22 (CH_2), 26.40 (CH_2), 48.55 ($\text{CH}_2\text{CH}=\text{CH}_2$), 59.72 (CH_2CH_3), 99.11 (SCH), 117.64 ($\text{CH}_2\text{CH}=\text{CH}_2$), 123.08 (Cq), 126.68 (Cq), 128.67 (CH Ar), 129.21 (CH Ar), 129.54 (CH Ar), 130.88 (Cq Ar), 134.21 (Cq), 138.06 (Cq), 140.51 (Cq), 161.45 (Cq), 164.45 (C=O).

4.1.3.16. (Z)-Isopropyl 2-((3-allyl-4-phenylthiazol-2(3H)-ylidene)amino)-4,5,6,7-tetrahydrobenzo[b]thiophene-3-carboxylate (**8d**)

Dark red oil. Yield: 65%. ^1H NMR (400 MHz, CDCl_3) δ 1.28 (6H, *d*, $J = 6.4$, CH_3), 1.75-1.84 (4H, *m*, CH_2), 2.67-2.70 (2H, *m*, CH_2), 2.75-2.78 (2H, *m*, CH_2), 4.62 (2H, *s*, $\text{CH}_2\text{CH}=\text{CH}_2$), 5.01 (1H, *d*, $J = 16.9$, $\text{CH}_2\text{CH}=\text{CH}_2$), 5.15 (1H, *d*, $J = 16.8$, $\text{CH}_2\text{CH}=\text{CH}_2$), 5.19 (1H, *m*, CH), 5.94 (1H, *ddt*, $J = 14.9, 6.8$ and 7.4 , $\text{CH}_2\text{CH}=\text{CH}_2$), 6.14 (1H, *s*, SCH), 7.36-7.40 (2H, *m*, CH Ar), 7.41-7.47 (3H, *m*, CH Ar). ^{13}C NMR (100 MHz, CDCl_3) δ 14.46 (CH_3), 22.87 (CH_2), 23.23 (CH_2), 25.23 (CH_2), 26.43 (CH_2), 48.44 ($\text{CH}_2\text{CH}=\text{CH}_2$), 59.60 (CH), 98.40 (SCH), 117.49 ($\text{CH}_2\text{CH}=\text{CH}_2$), 121.68 (Cq), 123.11 (Cq), 123.70 (Cq), 125.02 (Cq), 128.53 (CH Ar), 128.68 (CH Ar), 128.88 (CH Ar), 129.21 (CH Ar), 129.55 (CH Ar), 130.09 (Cq Ar), 130.88 ($\text{CH}_2\text{CH}=\text{CH}_2$), 132.38 (Cq), 134.23 (Cq), 140.55 (Cq), 164.46 (C=O).

4.2. Crystallography

Crystallographic data were collected on a Bruker diffractometer at 296 K. The frames were integrated with the Bruker SAINT software package using a narrow-frame algorithm. Data reduction and empirical absorption corrections

were carried out using the multi-scan method (SADABS). The structure was solved by direct methods and refined with SHELXS97 [31]. All non-H-atoms were refined anisotropically and H-atoms were constrained at their estimated positions using a riding model. The thermal ellipsoid diagram was generated with ORTEP3 [32]. The crystals were isolated from a tetrahydrofuran and hexane mixture at room temperature.

The fractional atomic coordinates and isotropic temperature parameters (\AA^2), the interatomic bond distances (\AA) and angles ($^\circ$) and the view of the packing showing the inter- and intramolecular interactions that stabilize the crystal structures for **9** and **8b** can be found in the supplementary material.

4.3. Cytotoxicity assay (MTT)

The cytotoxicity was evaluated using the enzymatic reduction of 3-(4,5-dimethylthiazol-2-yl)-2,5-diphenyltetrazolium bromide (MTT) assay to produce formazan crystals [33,34]. Cells (Macrophages J774) were seeded at 1.5×10^5 cells per well in 96-well plates in RPMI-1640 medium containing 10% fetal bovine serum for 16 hours. Cells were exposed to different concentrations of thiophene derivatives ($10\text{--}100 \mu\text{mol}\cdot\text{L}^{-1}$) dissolved in the vehicle (0.01%, DMSO) and maintained in culture for 24 hours at 37°C . At the end of the incubation in the presence of the samples, the cells were washed three times with PBS pH 7.4 and incubated with $100 \mu\text{L}$ of MTT solution ($5 \text{ mg}\cdot\text{mL}^{-1}$ in RPMI) for 4 h at 37°C . Following this incubation period, the supernatant was discarded and DMSO ($150 \mu\text{L}/\text{well}$) was added to each well to dissolve the formazan crystals. After 15 minutes at room temperature the absorbance was spectrophotometrically measured at 540 nm. Three individual wells were assayed per treatment and the results were expressed as percentage of cell viability ([absorbance of treated cells/absorbance of untreated cells] $\times 100$).

4.4. Biological evaluation

4.4.1. Assessment of compound activity against intracellular amastigotes

Trypanosoma cruzi CA-I/72 strain trypomastigotes were collected from the supernatant of infected C2C12 mice myocytes in T.75 culture flasks 7 days after the initial infection. The trypomastigotes were counted in a hemacytometer and their density was determined. A mixture containing 1.5×10^5 parasites and 1.0×10^4 C2C12 cells per milliliter of culture media was obtained and $50 \mu\text{L}$ was seeded per well in a 384-well plate with a clear bottom for microscopic imaging. Immediately after seeding the mixture of cells and parasites (1:15) we added 50 nL of the compounds, starting with a 10 mM stock solution, serially diluted. After three days of incubation the plate was fixed with the addition of $50 \mu\text{L}$ of 8% paraformaldehyde solution. We waited at least 1 hour to aspirate the well contents and added $0.5 \mu\text{g}\cdot\text{mL}^{-1}$ of DAPI for the staining of nucleic acid. After at least 3 hours of staining the plates were read in an ImageXpress Micro XL system (Molecular Devices) and images were analyzed using a dedicated algorithm developed in the MetaXpress software. Antiparasitic activity was normalized based on negative controls (untreated wells) and positive controls ($10 \mu\text{M}$ benznidazole). The host cell viability was based on the total number of host cells (C2C12) in each well relative to the average number of host cells from untreated wells (in percentage terms) [25].

4.4.2. Toxicity toward Y strain trypomastigotes

Trypomastigotes collected from the supernatant of LLC-MK2 cells were dispensed into 96-well plates at a cell density of 4.0×10^5 cells/well. Test inhibitors, dissolved in DMSO, were diluted

into five different concentrations, adjusted to $25 \mu\text{M}$ and added to the respective wells. The plate was then incubated for 24 hours at 37°C in 5% CO_2 . In the next step, propidium iodide ($400 \text{ ng}\cdot\text{mL}^{-1}$) was added and the test samples were incubated for 5 minutes. Aliquots of each well were collected and the number of viable parasites, based on parasite motility, was assessed in a Neubauer chamber. The percentage of inhibition was calculated in relation to untreated cultures. The IC_{50} was calculated using non-linear regression with the Prism 4.0 GraphPad software. Benznidazole was used as the reference drug [1,5].

4.4.3. Cruzain inhibition

Procruzain truncated at the C-terminal was expressed and purified using a modified protocol (Lee, Balouch and Craik, unpublished results). A $0.5 \text{ mg}/\text{mL}$ solution of procruzain (in 100 mM sodium acetate pH 5.5, 10 mM EDTA, 5 mM DTT and 1 M NaCl, pH adjusted to dialyzed in 10 mM Tris buffer pH 7.5, inhibited with the covalent reversible inhibitor methyl methanethiosulfonate (MMTS), and dialyzed again in the same buffer. Finally, the protein was purified in a MONO-Q anion exchange column, using 0 to 500 mM NaCl gradient in 10 mM Tris buffer (pH 7.5) [35].

Cruzain activity was measured by monitoring the cleavage of the fluorescent substrate Z-Phe-Arg-aminomethylcoumarin (Z-FR-AMC), in a Synergy 2 (Biotek) fluorimeter, at the Centre for Flow Cytometry Fluorimetry at the Department of Biochemistry and Immunology (UFMG). All assays were performed in the 96-well plate format, with a final volume of $200 \mu\text{L}$, in a buffer solution of 0.1 M sodium acetate pH 5.5 in the presence of 0.1 mM of betamercaptoethanol, 0.01% of Triton X-100, 0.5 nM of cruzain and $2.5 \mu\text{M}$ of substrate [26]. The assay was performed with and without the pre-incubation of the compounds with the enzyme. The initial screening was performed with $100 \mu\text{M}$ of the inhibitors, except for compounds **5d** and **8a**, which were assayed at 25 and $50 \mu\text{M}$, respectively, due to solubility limitations. For each assay, two independent experiments were performed, each in triplicate and monitored for 5 minutes. Enzymatic activity was calculated based on a comparison with a DMSO control, considering the initial reaction rate. E64 ($100 \mu\text{M}$) was used in the assay as a positive control. Since most compounds were observed to be time-dependent, which is consistent with a covalent mode of inhibition, all subsequent assays were performed with 10 minutes of pre-incubation. The IC_{50} curves were determined in two independent experiments, each involving at least nine compound concentrations, in triplicate. IC_{50} curves were determined with GraphPad Prism. The most potent compounds were further evaluated for detergent-sensitivity at different concentrations (0.01 and 0.1% Triton X-100) at a concentration close to its IC_{50} . The compound **7c** was also pre-incubated in the presence of $2 \text{ mg}\cdot\text{mL}^{-1}$ BSA to evaluate the formation of aggregates [26].

4.5. Molecular docking

For docking purposes, the three-dimensional structure of cruzain (PDB code: 1U9Q) was obtained from the RCSB protein databank. Ligands that were already present within the receptor in bound form were removed for the docking protocol. All of the ligands were prepared and docked for this study in flexible docking mode and atoms located within a range of 5.0 \AA from the amino acid residues were included in the active site. The docking calculations and minimization were carried out in the ArgusLab® module, with the Merck Molecular Force Field (MMFF), and most of the parameters had a set default with 10.000 cycles per molecule for the active site cavity.

For the preparation of the macromolecule, all heteroatoms, including water molecules, were deleted. Polar hydrogen atoms were added to the cruzain tree-dimensional structure. The partial atomic charges of the cruzain and thiophen-2-thiourea and 2-iminothiazolidine derivatives were then calculated using Kollman and Gasteiger-Marsili methods, respectively. The cruzain was placed inside a box with the number of center grid points in X x Y x Z directions being 2.77 x 10.289 x 6.45 and a grid spacing of 0.375 Å. Lamarckian genetic algorithms were employed to perform the docking calculations. The number of genetic algorithm runs and the number of evaluations were set to 100 and 2.5 million, respectively. For all other parameters default settings were used. For each of the docking cases, the lowest energy docked conformation, according to the AutoDock scoring function, was selected as the binding mode. Molecular models were built to discuss the binding modes by docking using an AutoDock Tools program.

Acknowledgments

This work was supported by the Conselho Nacional de Desenvolvimento Científico e Tecnológico (CNPq), Coordenação de Aperfeiçoamento de Pessoal de Nível Superior (CAPES) and Fundação de Amparo à Pesquisa do Estado de Alagoas (FAPEAL).

Supplementary Material

Supplementary material can be obtained free charge at doi:

References

- Moreira, D. R. M.; De Oliveira, A. D. T.; Teixeira De Moraes Gomes, P. A.; De Simone, C. A.; Villela, F. S.; Ferreira, R. S.; Da Silva, A. C.; Dos Santos, T. A. R.; Brelaz De Castro, M. C. A.; Pereira, V. R. A.; Leite, A. C. L. *Eur J Med Chem* **2014**, 75, 467.
- Gon, E.; Pereira, F.; Souza, D.; Augusto, R.; Sera, M.; Paula, A.; Loureiro, D. M.; Storpirtis, S.; Krogh, R.; De, A.; Carlos, L.; Igne, E. *Eur J Med Chem* **2014**, 82, 418.
- Papadopoulou, M. V.; Bloomer, W. D.; Rosenzweig, H. S.; Wilkinson, S. R.; Kaiser, M. *Eur J Med Chem* **2014**, 87, 79.
- Caputto, M. E.; Fabian, L. E.; Benítez, D.; Merlino, A.; Ríos, N.; Cerecetto, H.; Moltrasio, G. Y.; Moglioni, A. G.; González, M.; Finkielstein, L. M. *Bioorg Med Chem* **2011**, 19, 6818.
- Veríssimo, M.; Cardoso, D. O.; Rabelo, L.; Siqueira, P. De; Barbosa, E.; Bandeira, L.; Zaldini, M.; Rodrigo, D.; Carolina, M.; Brelaz, A.; Bernhardt, P. V.; Leite, A. C. L. *Eur J Med Chem* **2014**, 86, 48.
- Kryshchshyn, A.; Kaminsky, D.; Grellier, P.; Lesyk, R. *Eur J Med Chem* **2014**, 85, 51.
- Moreno-rodríguez, A.; Salazar-schettino, P. M.; Luis, J.; Torrens, H.; Guevara-g, Y.; Hern, F.; Pina-canseco, S.; Torres, M. B.; Cabrera-bravo, M.; Mendoza, C.; Eduardo, P. *Eur J Med Chem* **2014**, 87, 23.
- Martinez-Mayorga, K.; Byler, K. G.; Ramirez-Hernandez, A. I.; Terrazas-Alvares, D. E. *Drug Discov Today* **2015**, 20, 890.
- Saravanan, J.; Mohan, S.; Roy, J. J. *Eur J Med Chem* **2010**, 45, 4365.
- Neres, J.; Brewer, M. L.; Ratier, L.; Botti, H.; Buschiazzi, A.; Edwards, P. N.; Mortenson, P. N.; Charlton, M. H.; Alzari, P. M.; Frasc, A. C.; Bryce, R. A.; Douglas, K. T. *Bioorg Med Chem Lett* **2009**, 19, 589.
- Havrylyuk, D.; Zimenkovsky, B.; Karpenko, O.; Grellier, P.; Lesyk, R. *Eur J Med Chem* **2014**, 85, 245.
- Gewald, K.; Schinke, E.; Böttcher, H. *Chem Ber* **1966**, 99, 94.
- Arhin, F.; Bélanger, O.; Ciblat, S.; Dehbi, M.; Delorme, D.; Dietrich, E.; Dixit, D.; Lafontaine, Y.; Lehoux, D.; Liu, J.; McKay, G. a.; Moeck, G.; Reddy, R.; Rose, Y.; Srikumar, R.; Tanaka, K. S. E.; Williams, D. M.; Gros, P.; Pelletier, J.; Parr, T. R.; Far, A. R. *Bioorganic Med Chem* **2006**, 14, 5812.
- Nakhi, A.; Adepu, R.; Rambabu, D.; Kishore, R.; Vanaja, G. R.; Kalle, A. M.; Pal, M. *Bioorg Med Chem Lett* **2012**, 22, 4418.
- Cannito, A.; Perrissin, M.; Luu-Duc, C.; Huguet, F.; Gaultier, C.; Narcisse, G. *Eur J Med Chem* **1990**, 25, 635.
- Shih, M.-H.; Su, Y.-S.; Wu, C.-L. *Chem Pharm Bull (Tokyo)* **2007**, 55, 1126.
- Saiz, C.; Pizzo, C.; Manta, E.; Wipf, P.; Mahler, S. G. *Tetrahedron Lett* **2009**, 50, 901.
- Yella, R.; Ghosh, H.; Patel, B. K. *Green Chem* **2008**, 10, 1307.
- de Aquino, T. M.; Liesen, A. P.; da Silva, R. E. a.; Lima, V. T.; Carvalho, C. S.; de Faria, A. R.; de Araújo, J. M.; de Lima, J. G.; Alves, A. J.; de Melo, E. J. T.; Góes, A. J. S. *Bioorg Med Chem* **2008**, 16, 446.
- Pankova, A. S.; Samartsev, M. a.; Shulgin, I. a.; Golubev, P. R.; Avdontceva, M. S.; Kuznetsov, M. a. *RSC Adv* **2014**, 4, 51780.
- St. Laurent, D. R.; Gao, Q.; Wu, D.; Serrano-Wu, M. H. *Tetrahedron Lett* **2004**, 45, 1907.
- Devani, M. B.; Shishoo, C. J.; Pathak, U. S.; Parikh, S. H.; Shah, G. F.; Padhya, a C. *J Pharm Sci* **1976**, 65, 660.
- Litvinov, V. P. *Russ Chem Bull* **2004**, 53, 487.
- El-Baih, F. E. M.; Al-Blowy, H. a S.; Al-Hazimi, H. M. *Molecules* **2006**, 11, 498.
- Calvet, C. M.; Vieira, D. F.; Choi, J. Y.; Kellar, D.; Cameron, M. D.; Siqueira-Neto, J. L.; Gut, J.; Johnston, J. B.; Lin, L.; Khan, S.; McKerrow, J. H.; Roush, W. R.; Podust, L. M. *J Med Chem* **2014**, 57, 6989.
- Ferreira, R. S.; Bryant, C.; Ang, K. K. H.; McKerrow, J. H.; Shoichet, B. K.; Renslo, A. R. *J Med Chem* **2009**, 52, 5005.

27. de Souza, W.; de Carvalho, T. M. U.; Barrias, E. S. *Int J Cell Biol* **2010**, *2010*, 1.
28. Moreira, D. R. M.; Costa, S. P. M.; Hernandez, M. Z.; Rabello, M. M.; De Oliveira Filho, G. B.; De Melo, C. M. L.; Da Rocha, L. F.; De Simone, C. A.; Ferreira, R. S.; Fradico, J. R. B.; Meira, C. S.; Guimarães, E. T.; Srivastava, R. M.; Pereira, V. R. A.; Soares, M. B. P.; Leite, A. C. L. *J Med Chem* **2012**, *55*, 10918.
29. Cristina, A.; Leite, L.; Lima, R. S. De; Moreira, R. D. M.; Cardoso, D. O.; Gouveia, C.; Maria, L.; Hernandez, Z.; Kiperstok, C.; Santana, R.; Lima, D.; Soares, M. B. P. *Bioorg Med Chem* **2006**, *14*, 3749.
30. Feng, B. Y.; Shoichet, B. K. *Nat Protoc* **2006**, *1*, 550.
31. Sheldrick, G. M. *Acta Crystallogr Sect A Found Crystallogr* **2008**, *64*, 112.
32. Farrugia, L. J. *J Appl Crystallogr* **1997**, *30*, 565.
33. Berridge, M.; Tan, A.; McCoy, K.; Wang, R. *Biochemica* **1996**, *4*.
34. Mosmann, T. *J Immunol Methods* **1983**, *65*, 55.
35. Mott, B. T.; Ferreira, R. S.; Simeonov, A.; Jadhav, A.; Ang, K. K. H.; Leister, W.; Shen, M.; Silveira, J. T.; Doyle, P. S.; Arkin, M. R.; McKerrow, J. H.; Inglese, J.; Austin, C. P.; Thomas, C. J.; Shoichet, B. K.; Maloney, D. J. *J Med Chem* **2010**, *53*, 52.
36. Imre, G.; Veress, G.; Volford, A.; Farkas, Ö. *J Mol Struct THEOCHEM* **2003**, *666-667*, 51.
37. Halgren, T. A. *J Comput Chem* **1996**, *17*, 490.
38. Dewar, M. J. S.; Zuebisch, E. G.; Healy, E. F.; Stewart, J. J. P. *J Am Chem Soc* **1985**, *107*, 3902.
39. Metropolis, N.; Ulam, S. *J Am Stat Assoc* **2008**, *44*, 335.
40. Becke, A. D. *Phys Rev A* **1988**, *38*, 3098.
41. Spartan
http://www.wavefun.com/products/windows/SpartanModel/win_model.html **2015**.

Graphical Abstract

Design, synthesis, molecular docking and biological evaluation of thiophen-2-iminothiazolidine derivatives for use against *Trypanosoma cruzi*

Leave this area blank for abstract info.

Silva-Júnior, E.F.^a, Silva, E.P.S.^a, França, P.H.B.^a, Silva, J.P.N.^b, Barreto, E.O.^b, Silva, E.B.^c, Ferreira, R.S.^c, Gatto, C.C.^d, Moreira, D.R.M.^c, Siqueira-Neto, J.L.^f, Mendonça-Júnior, F.J.B.^g, Lima, M.C.A.^h, Bortoluzzi, J.H.ⁱ, Scotti, M.T.^g, Scotti, L.^g, Meneghetti, M.R.ⁱ, Aquino, T.M.*^a, Araújo-Júnior, J.X.^a

^aMedicinal Chemistry Laboratory, Pharmacy and Nursing School, Federal University of Alagoas, Maceio, Brazil. ^bCell Biology Laboratory, Federal University of Alagoas, Maceio, Brazil. ^cBiochemistry and Immunology Department, Biological Sciences Institute, Federal University of Minas Gerais, Belo Horizonte, Brazil. ^dInorganic Synthesis and Crystallography Laboratory, Institute of Chemistry, University of Brasília, Federal District, Brazil. ^eTissue Engineering and Immunopharmacology Laboratory, Oswaldo Cruz Foundation, Salvador, Bahia, Brazil. ^fSkaggs School of Pharmacy and Pharmaceutical Sciences, California, San Diego La Jolla, United States of America. ^gLaboratory of Drug Synthesis and Delivery, Biological Sciences Department, State University of Paraíba, Campus V, João Pessoa, Brazil. ^hDrug Design and Synthesis Laboratory, National Science and Technology Institute for Pharmaceutical Innovation, Federal University of Pernambuco, Recife, Brazil. ⁱCatalysis and Chemical Reactivity Group (GCaR), Institute of Chemistry and Biotechnology, Federal University of Alagoas, Maceio, Brazil

